

Article

# An Integrated Approach for Modeling Wetland Water Level: Application to a Headwater Wetland in Coastal Alabama, USA

Mehdi Rezaeianzadeh <sup>1,\*</sup>, Latif Kalin <sup>2</sup> and Mohamed M. Hantush <sup>3</sup>

<sup>1</sup> NOAA Affiliate, Lynker Technologies, Office of Water Prediction—Analysis and Prediction Division, NOAA National Water Center, Tuscaloosa, AL 35401, USA

<sup>2</sup> School of Forestry and Wildlife Sciences, Auburn University, 602 Duncan Drive, Auburn, AL 36849, USA; kalinla@auburn.edu

<sup>3</sup> National Risk Management Research Laboratory, U.S. Environmental Protection Agency, Cincinnati, OH 45268, USA; hantush.mohamed@epa.gov

\* Correspondence: mehdi.rezaeianzadeh@noaa.gov

Received: 18 May 2018; Accepted: 26 June 2018; Published: 2 July 2018



**Abstract:** Headwater wetlands provide many benefits such as water quality improvement, water storage, and providing habitat. These wetlands are characterized by water levels near the surface and respond rapidly to rainfall events. Driven by both groundwater and surface water inputs, water levels (WLs) can be above or below the ground at any given time depending on the season and climatic conditions. Therefore, WL predictions in headwater wetlands is a complex problem. In this study a hybrid modeling approach was developed for improved WL predictions in wetlands, by coupling a watershed model with artificial neural networks (ANNs). In this approach, baseflow and stormflow estimates from the watershed draining to a wetland are first estimated using an uncalibrated Soil and Water Assessment Tool (SWAT). These estimates are then combined with meteorological variables and are utilized as inputs to an ANN model for predicting daily WLs in wetlands. The hybrid model was used to successfully predict WLs in a headwater wetland in coastal Alabama, USA. The model was then used to predict the WLs at the study wetland from 1951 to 2005 to explore the possible teleconnections between the El Niño Southern Oscillation (ENSO) and WLs. Results show that both precipitation and the variations in WLs are partially affected by ENSO in the study area. A correlation analysis between seasonal precipitation and the Nino 3.4 Index suggests that winters are wetter during El Niño in Coastal Alabama. Analysis also revealed a significant negative correlation between WLs and the Nino 3.4 Index during the El Niño phase for spring. The findings of this study and the developed methodology/tools are useful to predict long-term WLs in wetlands and construct more accurate restoration plans under a variable climate.

**Keywords:** wetland hydrology; watershed models; ANN; climate variability; ENSO

## 1. Introduction

Headwater wetlands are among the most important wetland types in the coastal plains of the southeastern U.S. Since they are often the source of first and second order perennial streams, they act as natural filters for water quality improvements and therefore are crucial in protecting downstream aquatic systems [1]. Headwater wetlands are characterized by water tables at or near the surface that respond rapidly to rainfall events [2]. Driven by both groundwater and surface water inputs, water levels (WLs) can be above or below the ground at any given time, depending on the season and climatic conditions [3]; this dynamic behavior results in a highly complex ecosystem. The seasonal patterns of WLs in a wetland (i.e., hydroperiod) exhibit annual variation in response to climatic and

antecedent conditions [4]. Hence, long-term WL predictions can be a valuable source for evaluating these year to year variabilities. Furthermore, WL prediction and assessment are of great importance, especially in headwater wetlands since changing climate and land use/cover in watersheds draining to the wetlands affect WLs.

Wetlands are responsible for 20 to 25 percent of global methane emissions to the Earth's atmosphere, yet they also have the best capacity of any ecosystem to retain carbon through permanent burial (sequestration) [4] and sedimentation [5]. Among all eco-hydrologic indices, WL plays a key role in controlling CH<sub>4</sub> emissions by determining the interface between aerobic and anaerobic processes (above- vs. below-ground, respectively) [6] by regulating aerobic or anoxic conditions in sediments [7]. WL also determines the degree of CO<sub>2</sub> production [8,9]. All wetlands have both intra-annual (i.e., seasonal) and inter-annual (i.e., variation from year to year) WL fluctuations [10]. Such WL fluctuations have direct control on the composition of plants and animal communities/assemblages in wetlands [11]. Hodson et al. [12], demonstrated that climate variability has a significant impact on wetland CH<sub>4</sub> emissions. Studies have shown that rainfall and streamflow in the southeastern US are influenced by El Niño Southern Oscillation (ENSO) [13]. El Niño may also result in extreme weather events (e.g., droughts and cyclones) [14]. Headwater wetlands provide many benefits to Coastal Alabama and it is highly likely that their functioning (i.e., pollution reduction/water quality improvement, water storage and providing habitat to many animals and plants) are impacted by ENSO, which has not been investigated before. Thus, the potential impacts of climate variability on wetlands and their eco-hydrological characteristics are of great importance.

WLs in wetlands can be simulated by physically-based models (e.g., FEUWAnet by [15]; SWATRE by [16]; MIKE SHE by [17]) or empirical methods (e.g., [3]). While the former need information regarding soil, geomorphology, and hydrogeology of the system (draining watershed and wetland), which makes their development and application difficult particularly in data-scarce watersheds, the latter rely heavily on the hydro-climatic forcing (and their fluctuations) to the system. Artificial intelligence-based models such as artificial neural networks (ANNs) can be viable options where observed hydro-climatic data (e.g., inflow, outflow, water depth, precipitation, and temperature, etc.) exists but there is a lack of information on soil and hydrogeology of the system. Two examples of ANN applications in wetland hydrology studies are [18], and [3].

Transition in a watershed's land use and land cover (LULC) can alter groundwater recharge and surface runoff regimes. If the abutting uplands drain to a wetland, which is the case in headwater wetlands, these changes can adversely impact the wetland's hydrology [19]. Because of the land-use developments and increases in imperviousness in the watersheds draining to wetlands, headwater wetlands in time can become more of flow-through systems. Consequently, the retention time and the performance of the wetland in filtering pollutants can be altered. Evidence of such impacts and alterations of wetland hydrology have been reported by [20], and [21] in headwater wetlands of coastal Alabama. Nilsson et al. [22], pointed out that understanding the cumulative effects of wetlands at the watershed scale needs a good understanding of WL fluctuations. The need for incorporating groundwater/surface water components from contributing watersheds in wetland WL prediction studies is very clear.

To build a predictive model capable of capturing physical processes to some extent, coupling a watershed model with ANN would be useful. By running a watershed model, the hydrologic inputs from the contributing watershed to the wetland (i.e., slow and quick flow components) can be simulated. Input combinations to ANN play a crucial role in developing a robust model. In that sense, importing the baseflow and stormflow simulated by a watershed model as inputs to ANN can improve the accuracy of ANNs. To the best of authors' knowledge, no study has considered combining a watershed model with ANN to predict wetland WL, although there are studies that coupled watershed models and ANNs for streamflow prediction. For instance, Loukas and Vasiliades [23], coupled the University of British Columbia (UBC) watershed model with ANN to predict streamflow. Noori and Kalin [24], showed that combining ANN and watershed models can help overcome the limitations of each model and result in a stronger model for streamflow prediction. Also, Mekonnen et al. [25],

developed a hybrid modeling structure (by utilizing Soil and Water Assessment Tool SWAT and ANNs) to predict runoff generation from prairie landscapes.

We develop a coupled SWAT-ANN model in this paper to predict WLs in headwater wetlands. We then apply the model to a headwater wetland in coastal Alabama, USA to predict the WL at the deepest point of the wetland. The study wetland is a typical headwater wetland in Coastal Alabama and is representative of many in the region since this wetland is one of those 15 selected by Barksdale et al. [19], to properly represent the surrounding LULC of the region. Also, groundwater discharge (from surrounding uplands) is a major hydrologic input to these headwater wetlands [2]. Baseflow and stormflow estimates from the SWAT model were fed into the ANN model as forcing data to capture slow and quick flow components from the contributing watershed to the study wetland. Observed WL data were then used to train and test the ANN model. The coupled model of this paper overcomes some of the limitations of the two previously developed WL prediction models by Rezaeianzadeh et al. [3], which either required WL data from nearby wetlands (continuous model) or antecedent WL data from the target wetland itself (event based model) as input. None of those models are suited for long term predictions, which is needed to explore the impacts of climate variability on wetland hydrology. The utility of the developed model is demonstrated with an application, where we explored the potential teleconnections between El Niño Southern Oscillation (ENSO) and WL fluctuations in the study wetland. To the best of our knowledge, this study is the first attempt to look at the hydrologic function of a headwater wetland in Coastal Alabama under varying ENSO conditions. Although the WL data used to train and test the model was limited, the example application still provides some useful insights into the impact of climatic variability on WLs in the study wetland.

## 2. Study Area and Data Sets

The study wetland is located in Baldwin County, Alabama, USA (Figure 1). Mild winters and hot and humid summers are the main climatic characteristics of the region. Mean annual temperature and precipitation are 19.5 °C and 1650 mm, respectively. Headwater wetlands in coastal Alabama are groundwater driven and are usually located in the headwater reaches of first order streams [2]. Hummock/hollow microtopography and gradual slopes are the terrain characteristics. The soils of these wetlands are classified as “wet loamy alluvial lands” [26]. The study wetland is a representative of the headwater wetlands throughout southern Alabama. The soil consists of two main groups: Lv (i.e., local alluvial land; C) and Hb (i.e., Hyde, Bayboro, and Muck soils; A/D) [27]. Figure 1a shows the 15 headwater wetlands that have been originally studied by Barksdale et al. (2014). The minimum and maximum elevation of the study wetland is 7.12 m and 10.24 m, respectively. The study wetland is located within the Fish River watershed in the southwest portion of the county, which drains into Weeks Bay, a sub-estuary of Mobile Bay. The delineated watershed area (based on the outlet of the wetland) draining to the wetland is 83.57 ha with a mixed land use/cover (Figure 1b). Pasture/hay and evergreen forests are the dominant land uses in the watershed (Figure 1c). The dominant hydrologic soil groups are C (i.e., slow infiltration rate covering 41.3% of the area) and A (with high infiltration rate and 40% of the area), respectively. According to the information derived from National Wetlands Inventory (NWI), the study wetland is comprised of three sections, which includes the PFO1C (0.737 ha), PFO4C (0.485 ha), and PFO1C (0.314 ha) classification codes. These three sections are called Freshwater Forested/Shrub Wetland types by NWI and are classified as *inland* wetlands. Precipitation, minimum and maximum temperature data were obtained from the NOAA Robertsdale (USC00016988) climatic station. Wetland WLs (relative to the ground surface) were monitored at an hourly time scale at the deepest point of the wetland in shallow wells using In-Situ Mini-Troll 500 pressure transducers from February 2011 to March 2012 [19]. During the summer and fall (June through November) of 2011, drought conditions persisted across the study area with the driest period occurring from May–June [28]. However, there was no WL data available for the study wetland from 25 April 2011 to 17 July 2011 (Figure 2). Based on the long-term average of precipitation, five months including March, July, August, and September 2011 as well as February 2012 were above the average and the rest were below the average precipitation.

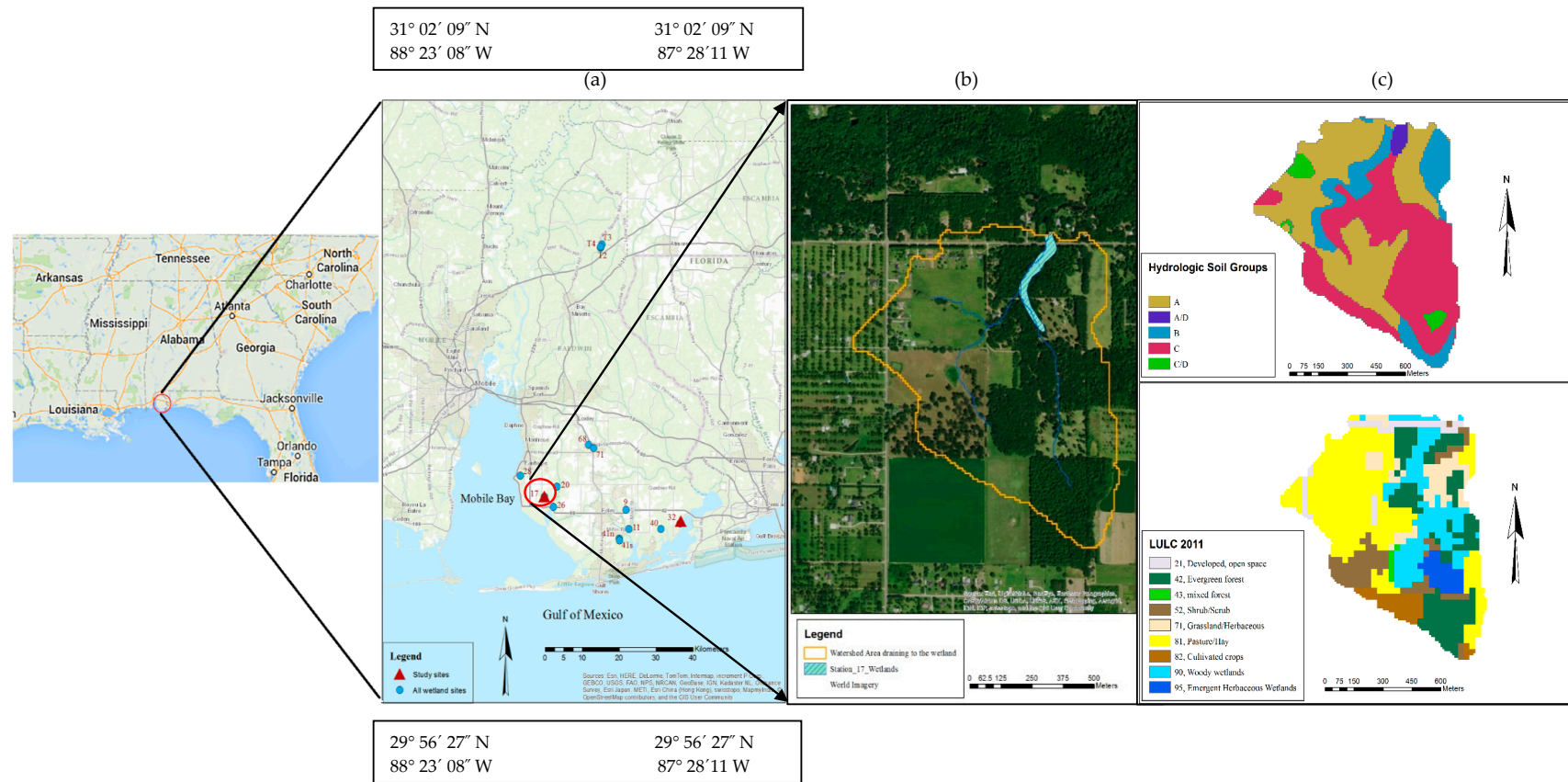


**Figure 1.** Study wetland with the delineated contributing watershed (a,b), and Hydrologic soil groups map and the land use/cover map based on 2011 National Land Cover Database (NLCD) for the study watershed (c).

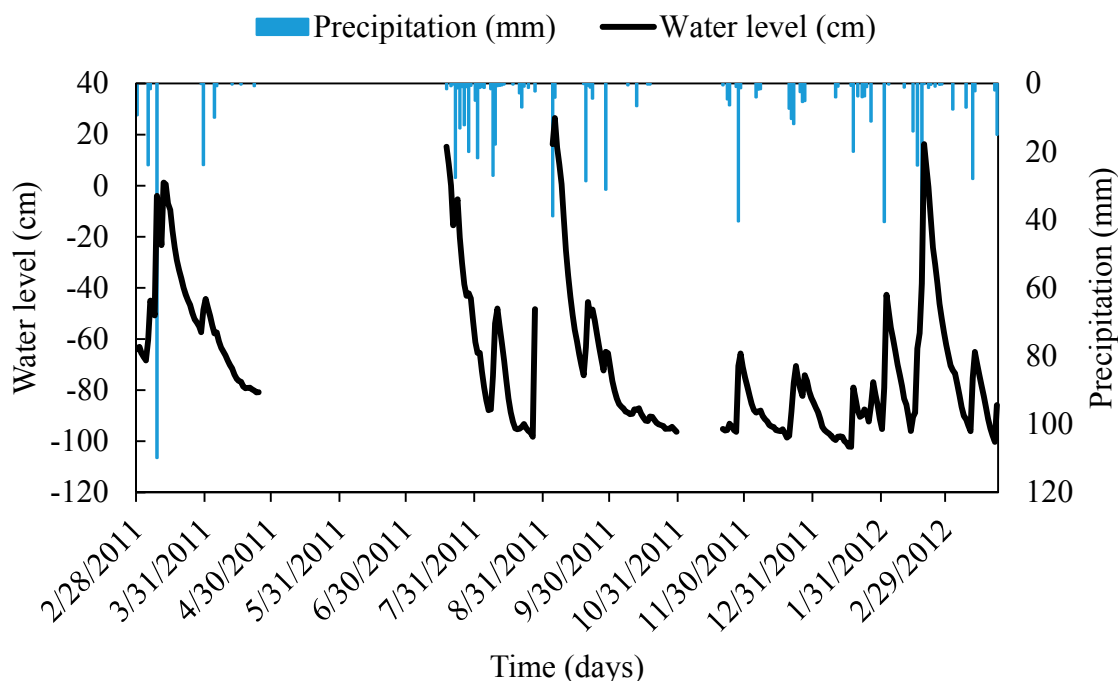


**Figure 2.** Water level recorded at the study wetland; there was no water level (WL) data available for the study wetland from 25 April 2011 to 17 July 2011. Note that there were two other periods of missing data for the study site. Altogether, water level data were available for 279 days.

### 3. Methodology

#### 3.1. Soil and Water Assessment Tool (SWAT)

SWAT is a semi-distributed, process-based watershed model that operates on a daily basis [29]. Division of a watershed into a number of subbasins is needed and done when different parts of the watershed are dominated by land uses or soils dissimilar enough to impact hydrology [30]. Hydrologic response units (HRUs) are lumped land areas within the subbasin that consist of unique land cover, soil, and management combinations [30]. In this study, the thresholds for land use, soil, and slope overlay, were all set to 10%, and the number of subbasins and HRUs were 5 and 74, respectively. The Soil Survey Geographic Database (SSURGO, [31]) was used to extract soil parameters. Land use/cover related data came from the 2011 National Land Cover Database (NLCD; [32]). Lu et al. [33] recommended Hamon method [34] for regional applications of potential evapotranspiration (PET) estimations in the southeastern United States. Thus, the Hamon method was used for the PET calculation, which utilizes daily mean air temperature. Daily average temperatures were obtained by simply averaging daily minimum and maximum temperatures. A three-year warm-up period was considered for SWAT run, and the daily baseflow and stormflow estimates generated from SWAT (no calibration) were regarded as two hydrologic inputs to the ANN model. Observed flow data (outflow from the watershed or inflow to the wetland) were not available for model calibration, which is commonly the case for many natural wetlands.

#### 3.2. Artificial Neural Networks (ANNs)

An ANN consists of a number of neurons organized into three basic layers (input, hidden, and output). The multilayer feed forward is one of the most common ANNs and it is therefore utilized in this study. Input combinations, the number of neurons in the hidden layer, transfer function, and training algorithms are the most important components of an ANN structure. The input combinations and transfer function are discussed in the following sections. For this study, average daily WLs were calculated from the hourly WL data, available from February 2011 to March 2012;

we obtained the best architecture to be (8, 6, 1). A simple trial and error procedure was carried out to find the best training algorithm and the Levenberg-Marquardt training algorithm was chosen for this study. A momentum constant (0 to 1) was used to avoid getting stuck in a local minimum [35]. Before applying the ANN models, the observed data were normalized to [0.05, 0.95] using a linear transformation [3,36]:

$$X_n = 0.05 + 0.9 \frac{X - X_{\min}}{X_{\max} - X_{\min}} \quad (1)$$

where,  $X_n$  and  $X$  are the normalized and original inputs and  $X_{\min}$  and  $X_{\max}$  are the minimum and maximum values of the original data, respectively.

The normalized data were employed to train the ANN model. The model outputs were then transformed back to the original scale and then the performance indices were computed for the training and test data sets. In this study, roughly 70% of the data was used for training and the remaining 30% was used for testing. To distribute the high, mean, and low WL values into both training and testing datasets, the data were randomly selected [3]. This randomization eliminates potential biases that may arise when there are distinct dry and wet periods. The randomization is done by randomly distributing the data into training and testing datasets until the  $p$ -value in the  $t$ -test is above 5%; i.e., there is no statistically significant difference between the means from the training and testing datasets. Note that the  $t$ -test is performed based on the equal variances assumption by conducting a Levene's test. The methodology is described in detail in Rezaeianzadeh et al. (2015) [3], therefore it is not repeated here. Previous exercises by Rezaeian-Zadeh et al. [36] and Rezaeianzadeh et al. [3] showed the efficiency of this method to optimally train the ANNs. The codes were written in MATLAB for the ANN simulation [37].

Although it is generally accepted that ANNs cannot extrapolate beyond the range of the training data [38], utilization of sigmoidal-type and linear transfer functions in hidden and output layers, respectively, has been recommended for extrapolation purposes [39,40]. For instance, Cigizoglu [41], and Rezaeian-Zadeh et al. [42], respectively showed the extrapolation ability of ANNs in predicting daily streamflows and hourly air temperatures. Hence, in the current study, logistic sigmoid and linear transfer functions were utilized in hidden and output layers, respectively. The logistic sigmoid transfer function is defined for a variable  $s$  as:

$$\text{logsig}(s) = \frac{1}{(1 + e^{-s})} \quad (2)$$

We utilized sigmoid and linear transfer functions for the hidden and output layers to build a more generalized model capable of capturing variations on unseen datasets including extrapolations. However, we need a longer dataset to increase the reliability of the developed model. Note that data limitation should not result in overlooking the capability of the introduced methodology in this study.

### 3.3. SWAT-ANN Coupling

To enhance WL predictions by the ANN model, a coupled SWAT-ANN model was developed. To that end, baseflow and stormflow components of streamflow are first simulated at the watershed outlet by the SWAT model without calibration (i.e., default SWAT parameter values are used). Note that even if they have a well-defined inlet, these wetlands typically receive surface and subsurface water from various points between the wetland inlet and outlet. Those dominantly un-regulated inflows to the wetlands impact the hydrology of these ecosystems in that area substantially. Hence, we decided to consider the outlet point of the wetland instead of the inlet point for SWAT analysis. This is achieved by picking the outlet of the wetland and delineating the watershed draining to that point as if there is no wetland there. Then, we generated streamflow at that point with SWAT using default model parameters. No calibration was carried out because streamflow data was not available. In addition to streamflow, SWAT also provides model outputs to help partition the streamflow into stormflow and baseflow components [30]. We did not separate baseflow from streamflow. SWAT

calculates baseflow, subsurface flow and surface runoff components. We considered surface runoff and subsurface flow as stormflow. We note that in many instances the wetland WLs are below the ground surface whereby groundwater bypasses the wetland and discharges directly to the main channel as baseflow. The simulated values for baseflow and stormflow at day  $t$  are then fed into ANN to predict WL on day  $t$ . A trial and error procedure was utilized to examine various input combinations, and their accuracies were evaluated with the Nash-Sutcliffe ( $E_{NS}$ ) and root mean square error ( $RMSE$ ) performance metrics. We evaluated the performance indices from both training and testing phases; however, the final input combination was decided based on the best validation matrices. To predict WL on day  $t$ , this combination was identified:

$$WL(t) = f\{Q_b(t), Q_b(t-1), Q_s(t), Q_s(t-1), P(t), P(t-1), PET(t), PET(t-1)\} \quad (3)$$

where,  $WL(t)$  is water depth at the deepest point in the wetland at time  $t$ ; and  $Q_b$ ,  $Q_s$ ,  $P$  and  $PET$  denote baseflow (i.e., groundwater contribution to streamflow), stormflow (or quick flow, i.e., surface runoff+interflow), precipitation, and potential evapotranspiration, respectively. These variables were found to serve as the best input combinations and were imported into ANN to predict WLs at their deepest point in the wetland for baseline and future periods. Figure 3 shows a flowchart describing the developed methodology of this study.

#### 3.4. El Niño Southern Oscillation (ENSO) Effects on WL Variations

Since rainfall and streamflow are influenced by ENSO in the southeastern US [13], one can also expect ENSO affecting WLs in wetlands. Because long-term observations are not available to study the impacts of climate variability, the developed SWAT-ANN model can be used to generate WLs in the study wetland. To predict WL from 1951 to 2005, observed data from the Fairhope 2 station (USC00012813), which is the nearest climatic station (<10 Km) with long-term historical data, from 1948 to 2005 were used to run the SWAT model. The SWAT model was run with a three-year warm-up period (1948–1950) from 1951 to 2005 to prepare the input data required for the trained ANN model. By importing baseflow and stormflow from the SWAT model, as well as precipitation and potential evapotranspiration to the trained ANN, WLs were predicted for this period (i.e., 1951–2005). The WLs predicted by the SWAT-ANN model over the period 1951–2005 were associated with ENSO indices to explore the existence of such a teleconnection at the study wetland. Several correlation methods are available to assess the strength of the relationship between large-scale atmospheric circulation patterns (such as ENSO) and hydro-climatic variables, but the two most commonly applied ones are Pearson's correlation and Spearman's rank correlation. Pearson's correlation needs both variables to be normally distributed while no such assumption is necessary for the application of Spearman's rank correlation [43]. For this study, Spearman's correlation coefficient between the Niño 3.4 index (as an indicator of ENSO strength) and the hydro-climatic variables precipitation and WL were examined. The Niño 3.4 index represents the sea-surface temperature (SST) anomalies in the Niño 3.4 region (5° N–5° S, 120–170° W) and is based on a 3-month running average [13]. The Niño 3.4 indices for the period 1951 to 2005 (to capture approximately 10 ENSO cycles) were obtained from the National Weather Service Climate Prediction Center.

When the Niño 3.4 index is between  $-0.5$  °C and  $0.5$  °C, it is considered to be a Neutral phase, and indices above  $0.5$  °C and below  $-0.5$  °C are listed as El Niño and La Niña phases of ENSO, respectively.

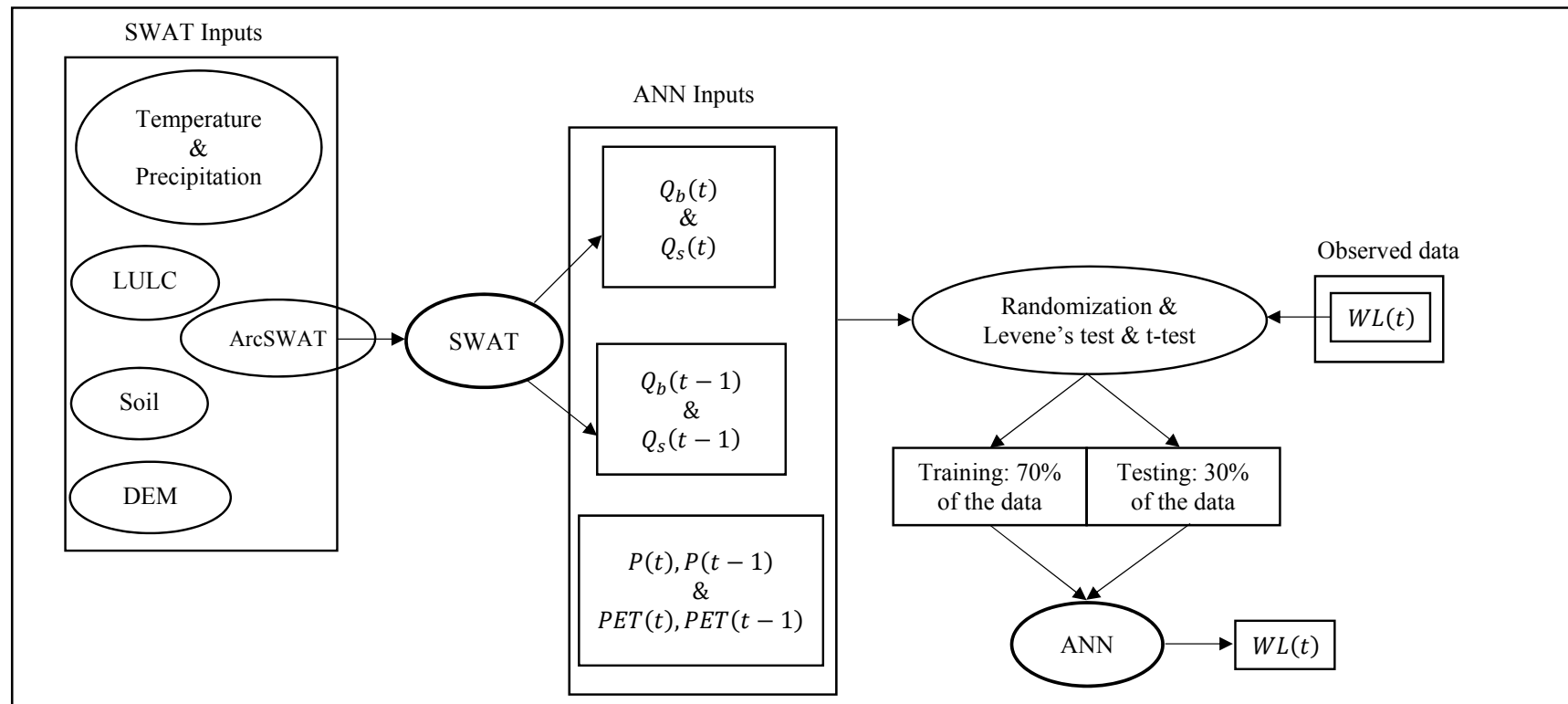


**Figure 3.** Model development flowchart.  $Q_b$ ,  $Q_s$ ,  $P$  and  $PET$  denote baseflow, stormflow, precipitation, and potential evapotranspiration, respectively. Data were randomly selected in which Levene's test and  $t$ -test (Rezaeianzadeh et al. [3]) were used to obtain the optimal datasets for training and testing phases.

## 4. Results

### 4.1. SWAT-ANN Model Performance

Figure 4 displays the simulated and observed daily average WLs for the training and testing phases in scatter plots and exceedance curves (i.e., probability of exceedance of “depth below ground surface”) formats. The  $E_{NS}$  and RMSE values were equal to 0.73, 14.5 cm, and 0.52, 17.8 cm, respectively, for the training and testing phases. Performance indices showed better results in the training phase compared to the testing phase, as expected. Better results regarding performance metrics were achieved too, but taking generalization and overfitting problems into consideration, the reported performances and the resulting model was the best and the most reliable.

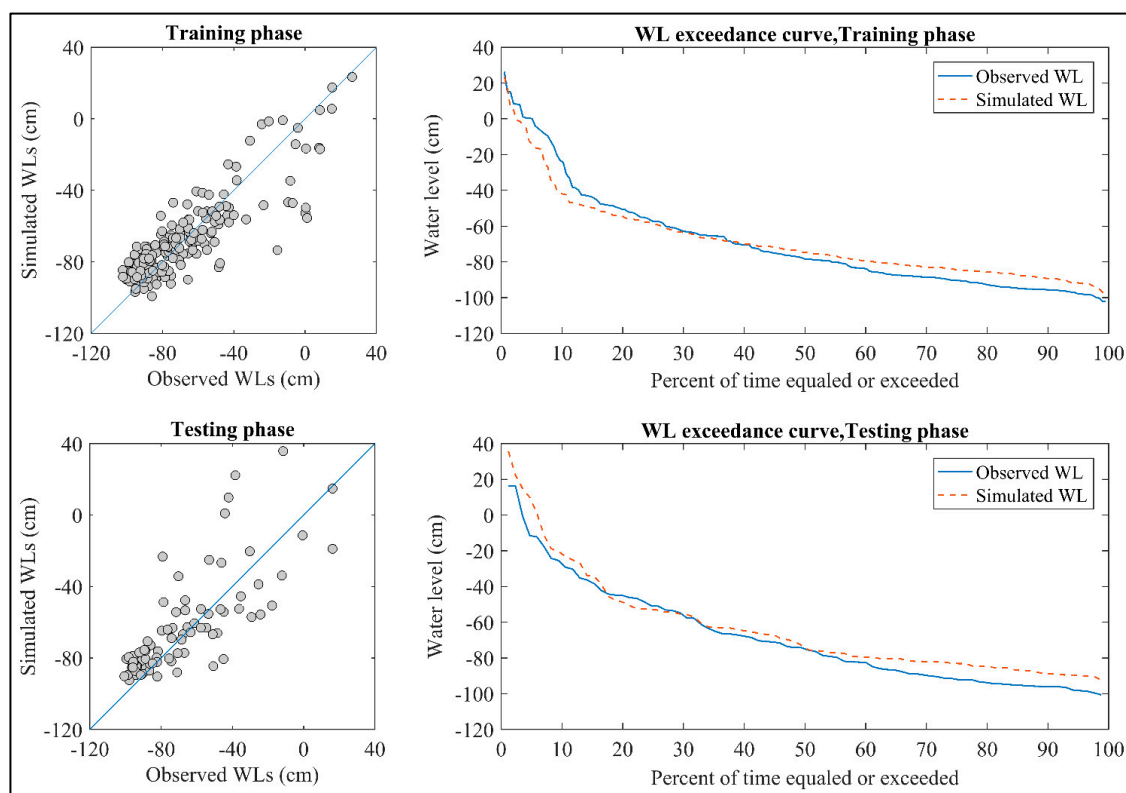


**Figure 4.** Simulated and observed daily average WLs for the training and testing phases in scatter plots and exceedance curves (i.e., probability of exceedance of “depth below ground surface”).

Although model performance metrics are not very high, as can be seen in Figure 4 the model has mostly captured the observed WL fluctuations well. Despite the model’s poor estimations of some extremely high WLs, the testing phase of Figure 4 also confirms the ability of the model to predict WLs accurately. The WL exceedance curve in Figure 4 regarding the training phase illustrates that in general, the model slightly overestimated WLs below  $-70$  cm. On the contrary, it slightly underestimated WLs above  $-60$  cm. Despite the results of the model in the training phase, the model in the testing phase overestimated the extreme high WLs. Similar to the training phase, WLs below  $-70$  cm were overestimated in the testing phase, too.

To utilize the developed model for long-term WL predictions, we elaborate on the generalization ability of the model. In making long-term predictions, some extreme values may be observed beyond the range of available time series used for model training, which would require paying attention to the generalization ability of the ANNs. The generalization ability including both interpolations and extrapolations is defined as the model’s skill to perform well on a dataset that is not utilized

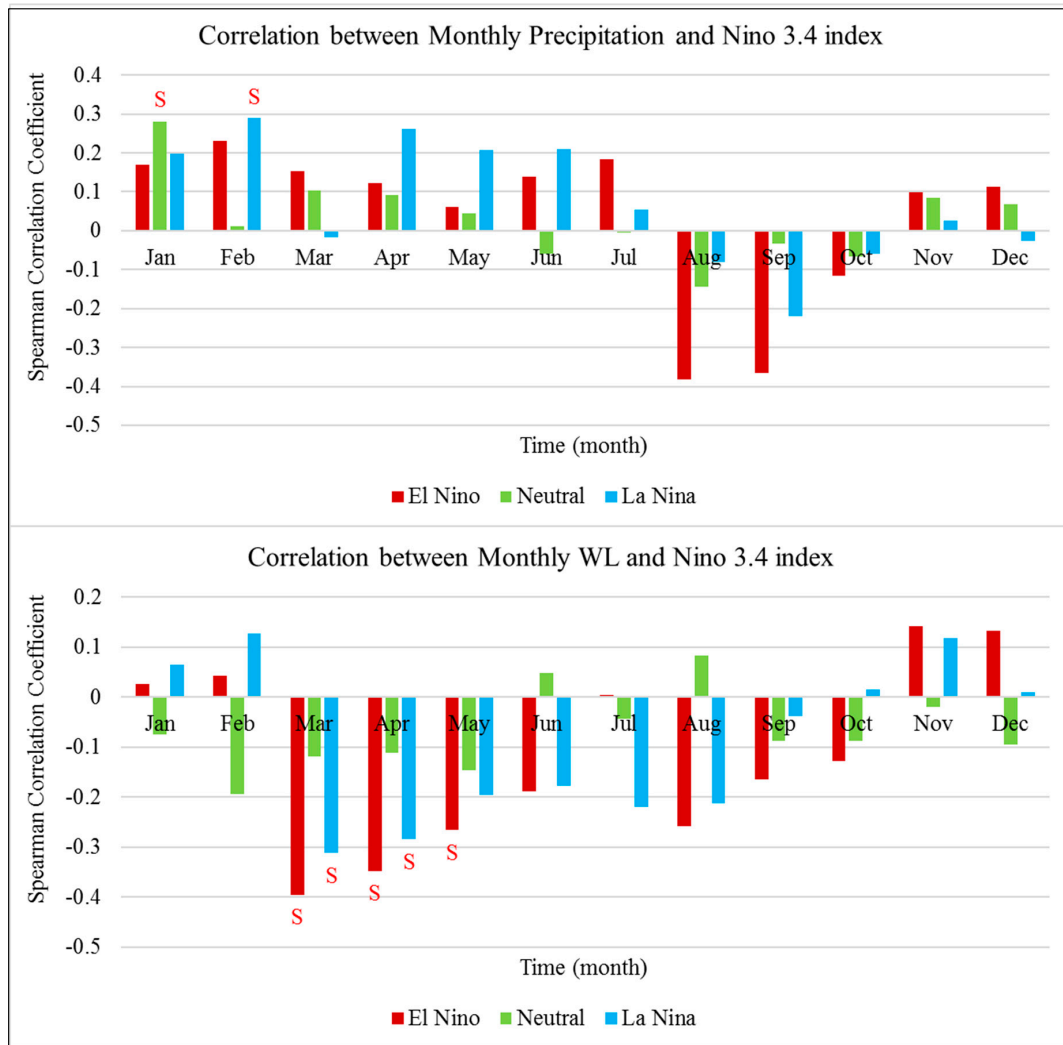
for its calibration [44]. Although it is generally accepted that the ANNs cannot extrapolate beyond the range of the training data [38], utilization of sigmoidal-type, and linear transfer functions in hidden and output layers, respectively, has been recommended for extrapolation purposes [39,40]. For instance, Rezaeian-Zadeh et al. [42], successfully tested the generalization ability of ANNs to predict hourly air temperatures by using the same type of transfer functions. The other successful example of the extrapolation ability of ANNs (compared to multi non-linear regression) was reported by Cigizoglu [41], on daily river flow data. Hence, in the current study, logistic sigmoid and linear transfer functions were utilized in hidden and output layers, respectively.

Generalization ability is also defined as a function of the ratio of the number of training samples to the number of connection weights. If this ratio is too small, continued training can result in overfitting of the training data [36]. Overfitting (i.e., having high variance) can happen when there are too many features (i.e., inputs) but insufficient amounts of observed data; in which case the learned hypothesis may fit the training set very well, but fail to generalize to new datasets. For this study, we obtained the best architecture to be (8, 6, 1), where those values refer to the number of inputs, and the number of neurons in hidden and output layers, respectively. Hence, we had  $8 \times 195$  (=1560; 195 corresponds to 70% of daily WL data used in the training phase) training patterns (samples), 54 weights and  $(6 + 1 = 7)$  "bias" weights, which constitute a total of 61 connection weights (i.e., free model parameters). Hence, the ratio for the developed model in this study was higher than 25, which confirms a reliable ANN with regard to the generalization ability and overfitting problem. To ensure a good generalization ability, various ratios have been suggested by researchers such as 2 to 1 [45], or 10 to 1 (e.g., [46]). Amari et al. [47], suggested that overfitting does not occur if the above ratio exceeds 30.

#### 4.2. Teleconnection between ENSO and WLs

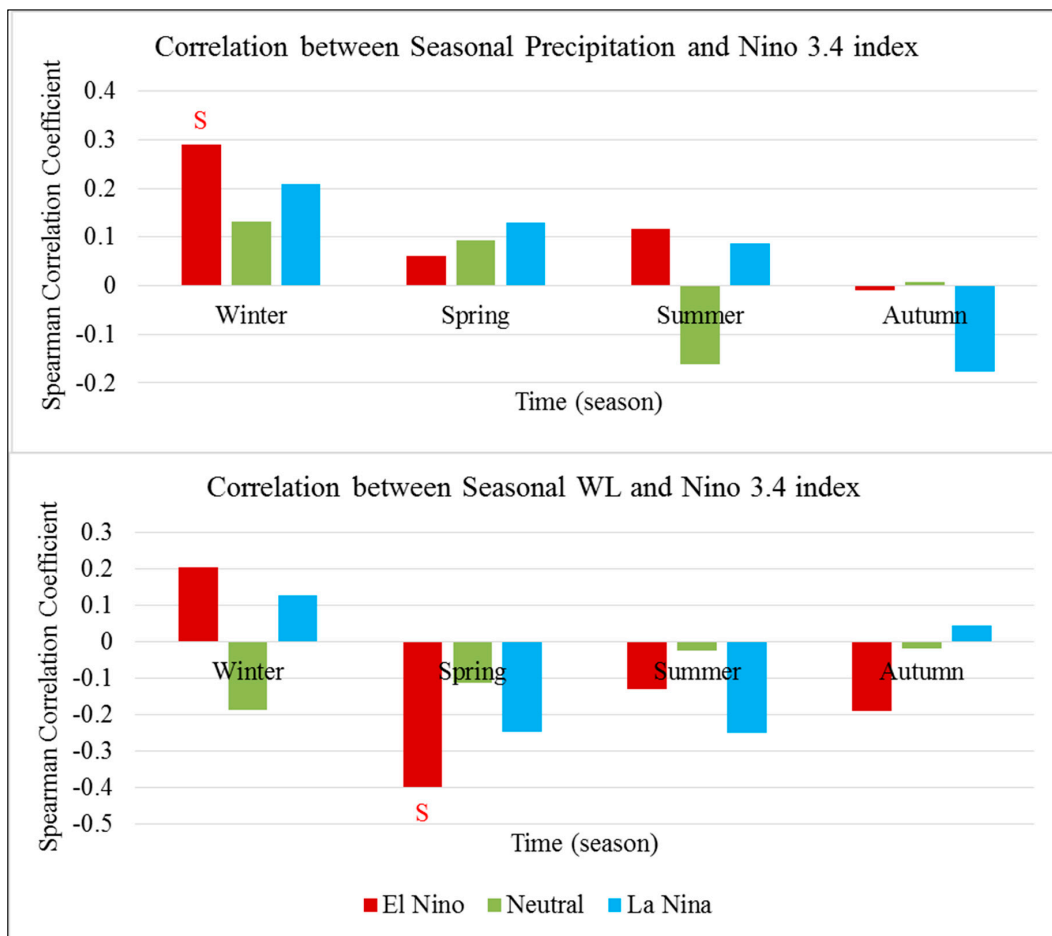
We had only one year of data to train and test the ANN model. Although model performance during both phases are good, the shortness of the data period used in training the model is still a limitation of the model and potentially raises a question on the reliability of extrapolation. Therefore, the results presented below should be interpreted with caution. Note that there are many successful ANN applications in hydrology in the literature with similarly short data (e.g., [48,49]). This fact was acknowledged by the ASCE Task Committee on Application of the ANNs in Hydrology (ASCE 2000) as "Very often, we may have no alternative but to proceed with limited data."

Figure 5 displays the Spearman's correlation coefficient between the Niño 3.4 index (as an indicator of ENSO strength) and monthly precipitation and WLs from 1951 to 2005. In August, September, and October, monthly precipitations are negatively correlated with the Niño 3.4 index in all three phases, but not at a statistically significant level ( $\alpha = 5\%$ ). From November to July, the correlations between monthly precipitations and the Niño 3.4 index are positive for almost all months and phases. However, only January in the neutral phase ( $p$ -value = 0.036) and February in the La Niña phase ( $p$ -value = 0.030) had statistically significant correlations (approximately  $r = 0.28$  for both cases). Average monthly WLs in March and April have a statistically significant negative correlation with the Niño index in both El Niño and La Niña phases, with a stronger correlation with the former. WLs in May also showed significant negative correlation with the Niño index in an El Niño phase. There are no statistically significant correlations between monthly WLs and the Niño index during the neutral phase.



**Figure 5.** Spearman’s correlation coefficient between the Niño 3.4 index and precipitation (**top** figure) and WL (**bottom** figure) in monthly scale. S indicates the significant correlations at 95% confidence level.

Figure 6 displays the Spearman correlation coefficients between the Niño index and precipitation/WL at the seasonal level. Correlations between the Niño index representing various ENSO phases and seasonal precipitations are non-significant except for a positive correlation in winter during the El Niño phase. This also aligns with what others reported (e.g., [50,51]). Correlations between the Niño index and seasonal WLs are non-significant except for spring during the El Niño phase, which has a negative correlation. Hence, lower WLs can be expected during the El Niño phase in spring. In late spring, Alabama is anomalously dry during the resurgence phase of El Niño. In the late spring of a developing El Niño, low-level winds that bring moist air from the Gulf of Mexico to the U.S. shift westward [52], which again confirms having less precipitation (than normal). Mearns et al. [53], found that precipitation over the southeastern U.S. shows different seasonality over the region.



**Figure 6.** Spearman correlation coefficients between the El Niño Southern Oscillation (ENSO) phases and precipitation/WL at seasonal scale.

### 5. Discussion

Headwater wetlands of coastal Alabama have two distinct aspects: (i) they respond quickly to rainfall events, which represent the stormflow component, and (ii) they are groundwater driven in which this component apparently plays a crucial rule in these ecosystems. The idea behind the coupled hybrid model was to capture the hydrologic inputs from the contributing watershed to the study wetland. In this way and by utilizing the SWAT model, which partitions the simulated flows into stormflow and baseflow, we gained better insight into the hydrology in the study wetland. To elaborate more on this, spring precipitation and WL can be a typical example of the situation. There is a (low) positive correlation between spring precipitation and the Niño index in an El Niño phase and while one can expect to see an increase (although insignificant) in the spring WLs, this is not the case here. Spring WLs have been probably affected more by the lagged response of subsurface hydrology and groundwater recharge to decreased precipitation at the end of summer during the El Niño phase and early autumn than spring precipitation.

The developed hybrid model in this study requires neither WL data from nearby wetlands nor antecedent WL data from the target wetland itself as input, which makes it practical for long term predictions. To the best of the authors’ knowledge, the developed methodology in this study is the first of its own in wetland hydrology studies, which feeds the simulated surface and groundwater components from a semi-distributed watershed hydrology model (SWAT) with a neural network model.

Slight changes in wetland hydrologic conditions can affect soil biogeochemistry and consequently nutrient cycles; biota may respond with considerable changes in species composition and richness and in ecosystem productivity [4]. In forested wetlands, hydrologic changes can also have substantial effects on forest productivity and carbon cycling [18], directly through duration, intensity, and frequency of flooding, and through changes in vegetation [54]. Barksdale et al. [18], found a strong correlation between WL and the total carbon content at the soil surface using data from 15 headwater wetlands (which included the wetland studied in this paper). According to their findings, wetlands with lower median groundwater levels showed surface soils with less organic matter and reduced carbon storage. WLs are expected to drop in spring during El Niño in the study wetland and this will potentially lead to reduced organic material and carbon stock and the same impacts could be expected in the other headwater wetlands of Baldwin County, Alabama. Reduction in WLs could also result in changes in the vegetation communities since the depth and percentage of time a location remains inundated has been shown to have a direct influence on the vegetative communities [55]. This could cause the establishment of invasive plant species, which are major threats to local diversity and other ecosystem functions [20]. With lowered WLs and the consequent increase in oxygen availability, a reduction in CH<sub>4</sub> emission and an increase in CO<sub>2</sub> production will be the most probable scenarios expected. With respect to the CH<sub>4</sub> emission, Zhu et al. [56], concluded that an El Niño event can trigger water table reduction and increased CH<sub>4</sub> soil consumption, leading to a reduction in CH<sub>4</sub> emission from tropical wetlands. Hydrologic alteration of headwater wetlands has the potential to impact some wildlife species, but the most severe impacts would be to amphibians since they are highly vulnerable to wetland drainage [2].

In this study, the potential impacts of climate variability on wetlands through alteration in one of the hydrologic indices (i.e., wetland water level) were discussed only. Other climate-related variables could have noticeable impacts such as increased temperature and altered evapotranspiration, altered biogeochemistry, altered amount and patterns of suspended sediment loadings and fire [57]. Also, human-induced alterations (which were beyond the scope of this study) including wetland drainage, filling/dredging, water diversions, introducing pollutants, and unsustainable developments need to be taken into account in the evaluation of potential impacts on wetlands and to avoid the detrimental impacts of these significant stressors.

## 6. Summary and Conclusions

Predicting WLs in wetlands where the hydrology is controlled by both surface runoff and groundwater is a challenging task. Acquiring knowledge about the probable changes in long-term WL fluctuations in wetlands and identifying their trends are even more complicated because of the complexity of hydrological processes in these ecosystems. In this study, we built upon the study of Rezaeianzadeh et al. [3], where the need for WL data from nearby wetlands as inputs to the model has been eliminated. Using simulated baseflow and stormflow components from the SWAT model run by default model parameters as hydrologic inputs to an ANN, this semi-distributed watershed hydrology model was externally coupled with an ANN. Although coupling data-driven models with semi-distributed hydrologic models (such as SWAT) are not new, to the best of the authors' knowledge, the developed model for the prediction of daily WLs is a novel approach in wetland hydrology studies. The ANN component of the hybrid model requires only the WL measurements over a certain period of time for training of the ANN.

The utility of the proposed model was demonstrated in a headwater wetland in coastal Alabama. The model performance statistics  $E_{NS}$  and  $RMSE$  were 0.73 and 14.5 cm, respectively, for the training phase, and 0.52 and 17.8 cm, respectively, for the testing phase. We had only one year of data to train and test the ANN model, and with this limited amount of data the model had good skill in predicting WLs. We acknowledge that although the availability of a longer wetland WL data series is desirable to better demonstrate the reliability of the developed model, the length of the WL data record was limited in this study and thus was the only option to gain some insights into the variations in the WLs

in the study wetland. To illustrate the potential use of wetland WL prediction, the developed hybrid model was used to generate WLs for the period 1951–2005 to explore the potential teleconnections between ENSO and WLs in the study wetland.

In summary, the following conclusions are drawn from this study:

- Coupled SWAT-ANN model was proved to be a viable tool to simulate WLs for wetlands at a daily time scale. By examining the ratio of the number of training samples to the number of connection weights, the model development was conducted cautiously to avoid the overfitting problem that is commonly ignored in the application of machine learning techniques in the hydrology and water resources field. Note that there are more sophisticated techniques to avoid overfitting, such as adding regularization to the cost function, and dropout regularization [58], but those have not been considered in this study.
- Correlations between the Niño index representing various ENSO phases and seasonal precipitations were non-significant at the study wetland, except for a positive correlation in winter during the El Niño phase. Correlations between the Niño index and seasonal WLs were non-significant, except for spring during the El Niño phase, which had a negative correlation. Hence, the findings suggest that winter gets wetter with regards to precipitation and spring gets drier in terms of WL over the El Niño phase in the study area.
- The teleconnection between WLs and ENSO phases shown in this study can also have important implications for the wetland vegetation and the functioning of wetlands. Specifically, in our study wetland, a reduction in WLs are expected in spring during El Niño and this would potentially lead to reduced organic material and carbon stock and the same impacts could be expected in the other headwater wetlands of Baldwin County, Alabama.

The methodology proposed in this paper should be transferable to other wetlands and their draining watersheds within different geographic and climatic regions to evaluate probable WL fluctuations in response to climatic variations. Studies such as the one presented in this paper are important in order to understand the potential hydrological changes associated with climate variability. These findings are of interest to wetland scientists, eco-hydrologists, wetlands managers, as well as domestic/international policy makers.

**Author Contributions:** Conceptualization, M.R. L.K. and M.M.H.; Methodology, M.R. and L.K.; Software, M.R.; Validation, M.R.; Formal Analysis, M.R. and L.K.; Investigation, M.R. and L.K.; Resources, L.K.; Data Curation, M.R.; Writing-Original Draft Preparation, M.R.; Writing-Review & Editing, M.R., L.K. and M.M.H.; Visualization, M.R.; Supervision, L.K. and M.M.H.; Project Administration, L.K. and M.M.H.; Funding Acquisition, L.K.

**Funding:** This study was partially funded by the U.S. Environmental Protection Agency (EPA) and Auburn University Center for Environmental Studies at the Urban-Rural interface (CESURI).

**Acknowledgments:** The authors would like to thank Christopher J. Anderson and W. Flynt Barksdale for the water level data. This paper has not been subject to the U.S. EPA review and therefore does not necessarily reflect the views of the Agency, and no official endorsement should be inferred.

**Conflicts of Interest:** The authors declare that they have no conflict of interest.

## References

1. Savage, R.; Baker, V. The Importance of Headwater Wetlands and Water Quality in North Carolina. 2007. Available online: <http://water.epa.gov/type/wetlands/assessment/survey/presentations.cfm> (accessed on 10 January 2015).
2. Noble, C.V.; Wakeley, J.S.; Roberts, T.H.; Henderson, C. *Regional Guidebook for Applying the Hydrogeomorphic Approach to Assessing the Functions of Headwater Slope Wetlands on the Mississippi and Alabama Coastal Plains*; U.S. Army Corps of Engineers: Washington, DC, USA, 2007.
3. Rezaeianzadeh, M.; Kalin, L.; Anderson, C. Wetland Water-Level Prediction Using ANN in Conjunction with Base-Flow Recession Analysis. *J. Hydrol. Eng.* **2015**, *22*, D4015003. [CrossRef]
4. Mitsch, W.J.; Gosselink, J.G. *Wetlands*, E-book. 2015. Available online: <http://auburn.ebilib.com/patron/FullRecord.aspx?p=1895927> (accessed on 16 November 2015).

5. Ouyang, X.; Lee, S.Y. Updated estimates of carbon accumulation rates in coastal marsh sediments. *Bioesciences* **2014**, *11*, 5057–5071. [[CrossRef](#)]
6. Kang, H.; Jang, I.; Kim, S. Key processes in CH<sub>4</sub> dynamics in wetlands and possible shifts with climate change. In *Global Change and the Function and Distribution of Wetlands*; Middleton, B.A., Ed.; Springer: New York, NY, USA, 2012; pp. 99–114.
7. Ouyang, X.; Lee, S.Y.; Connolly, R.M. Structural equation modelling reveals factors regulating surface sediment organic carbon content and CO<sub>2</sub> efflux in a subtropical mangrove. *Sci. Total Environ.* **2017**, *578*, 513–522. [[CrossRef](#)] [[PubMed](#)]
8. Daulat, W.E.; Clymo, R.S. Effects of temperature and watertable on the efflux of methane from peatland surface cores. *Atmos. Environ.* **1998**, *32*, 3207–3218. [[CrossRef](#)]
9. Chimner, R.A.; Cooper, D.J. Influence of water table levels on CO<sub>2</sub> emissions in a Colorado subalpine fen: An in situ microcosm study. *Soil Biol. Biochem.* **2003**, *35*, 345–351. [[CrossRef](#)]
10. McVoy, C.W.; Said, W.P.; Obeysekera, J.; Van Arman, J.A.; Dreschel, T.W. *Landscapes and Hydrology of the Predrainage Everglades*; University Press of Florida: Gainesville, FL, USA, 2011.
11. Van der Valk, A.; Volin, J.; Wetzel, P. Predicted changes in interannual water-level fluctuations due to climate change and its implications for the vegetation of the Florida Everglades. *Environ. Manag.* **2015**, *55*, 799–806. [[CrossRef](#)] [[PubMed](#)]
12. Hodson, E.L.; Poulter, B.; Zimmermann, N.E.; Prigent, C.; Kaplan, J.O. The El Niño-Southern Oscillation and wetland methane interannual variability. *Geophys. Res. Lett.* **2011**, *38*, L08810. [[CrossRef](#)]
13. Singh, S.; Srivastava, P.; Abebe, A.; Mitra, S. Baseflow response to climate variability induced droughts in the Apalachicola–Chattahoochee–Flint River Basin, U.S.A. *J. Hydrol.* **2015**, *528*, 550–561. [[CrossRef](#)]
14. Ouyang, X.; Lee, S.Y.; Connolly, R.M.; Kainz, M.J. Spatially-explicit valuation of coastal wetlands for cyclone mitigation in Australia and China. *Sci. Rep.* **2018**, *8*, 3035. [[CrossRef](#)] [[PubMed](#)]
15. Dall’O, M.; Kluge, W.; Bartels, F. FEUWAnet: A multi-box water level and lateral exchange model for riparian wetlands. *J. Hydrol.* **2001**, *250*, 40–62. [[CrossRef](#)]
16. Spieksma, J.F.M.; Schouwenaars, J.M. A simple procedure to model water level fluctuations in partially inundated wetlands. *J. Hydrol.* **1997**, *196*, 324–335. [[CrossRef](#)]
17. House, A.R.; Thompson, J.R.; Acreman, M.C. Projecting impacts of climate change on hydrological conditions and biotic responses in a chalk valley riparian wetland. *J. Hydrol.* **2016**, *534*, 178–192. [[CrossRef](#)]
18. Dadaser-Celik, F.; Cengiz, E. A neural network model for simulation of water levels at the Sultan Marshes wetland in Turkey. *Wetlands Ecol. Manag.* **2013**, *21*, 297–306. [[CrossRef](#)]
19. Barksdale, W.F.; Anderson, C.J.; Kalin, L. The influence of watershed run-off on the hydrology, forest floor litter and soil carbon of headwater wetlands. *Ecohydrology* **2014**, *7*, 803–814. [[CrossRef](#)]
20. Barksdale, W.F. The Effect of Land Use/Land Cover on Headwater-Slope Wetlands in Baldwin County, Alabama. Master’s Thesis, Auburn University, Auburn, AL, USA, 2013.
21. Barksdale, W.F.; Anderson, C.J. The influence of land use on forest structure, species composition, and soil conditions in headwater-slope wetlands of coastal Alabama, USA. *Int. J. Biodivers. Sci. Ecosyst. Serv. Manag.* **2014**. [[CrossRef](#)]
22. Nilsson, K.A.; Rains, M.C.; Lewis, D.B.; Trout, K.E. Hydrologic characterization of 56 geographically isolated wetlands in west-central Florida using a probabilistic method. *Wetlands Ecol. Manag.* **2013**, *21*, 1–14. [[CrossRef](#)]
23. Loukas, A.; Vasilades, L. Streamflow simulation methods for ungauged and poorly gauged watersheds. *Nat. Hazards Earth Syst. Sci.* **2014**, *14*, 1641–1661. [[CrossRef](#)]
24. Noori, N.; Kalin, L. Coupling SWAT and ANN Models for Enhanced Daily Streamflow Prediction. *J. Hydrol.* **2016**, *533*, 141–151. [[CrossRef](#)]
25. Mekonnen, A.; Nazemi, A.; Mazurek, K.A.; Elshorbagy, A.; Putz, G. Hybrid modelling approach to prairie hydrology: Fusing data-driven and process-based hydrological models. *Hydrol. Sci. J.* **2015**, *60*, 1473–1489. [[CrossRef](#)]
26. McBride, E.H.; Burgess, L.H. Soil survey of Baldwin County, Alabama. U.S. Department of Agriculture. Soil Conservation Service. *Soil Surv. Rep.* **1964**, *12*, 110.
27. USDA Web Soil Survey. Available online: <https://websoilsurvey.nrcs.usda.gov> (accessed on 9 January 2018).
28. National Climatic Data Center. Available online: <http://www.ncdc.noaa.gov/statistical-weather-and-climate-information> (accessed on 15 December 2012).

29. Arnold, J.G.; Srinivasan, R.; Muttiah, R.S.; Williams, J.R. Large area hydrologic modeling and assessment: Part I. Model development. *J. Am. Water Resour. Assoc.* **1998**, *34*, 73–89. [[CrossRef](#)]
30. Neitsch, S.L.; Arnold, J.G.; Kiniry, J.R.; Williams, J.R. Soil and water assessment tool: Theoretical documentation, version 2009. In *Grassland, Soil and Water Research Laboratory-Agricultural Research Service*; Blackland Research Center, Texas AgriLife Research: Temple, TX, USA, 2011; 647p.
31. Soil Survey Geographic Database (SSURGO). Available online: [https://www.nrcs.usda.gov/wps/portal/nrcs/detail/soils/survey/?cid=nrcs142p2\\_053627](https://www.nrcs.usda.gov/wps/portal/nrcs/detail/soils/survey/?cid=nrcs142p2_053627) (accessed on 9 January 2018).
32. National Land Cover Database (NLCD). Available online: <https://www.mrlc.gov/nlcd2011.php> (accessed on 9 January 2018).
33. Lu, J.; Sun, G.; Amatya, D.M.; McNulty, S.G. A Comparison of six potential evapotranspiration methods for regional use in the southeastern United States. *J. Am. Water Resour. Assoc.* **2005**, *41*, 621–633. [[CrossRef](#)]
34. Hamon, W.R. Estimating potential evapotranspiration. *J. Hydraul. Div. Proc. Am. Soc. Civ. Eng.* **1961**, *871*, 107–120.
35. Vogl, T.P.; Mangis, J.K.; Rigler, A.K.; Zink, W.T.; Alkon, D.L. Accelerating the convergence of the backpropagation method. *Biol. Cybern.* **1998**, *59*, 256–264.
36. Rezaeian Zadeh, M.; Amin, S.; Khalili, D.; Singh, V.P. Daily outflow prediction by multilayer perceptron with logistic sigmoid and tangent sigmoid activation functions. *Water Resour. Manag.* **2010**, *24*, 2673–2688. [[CrossRef](#)]
37. MathWork, Inc. *Matlab User's Manual*, version 7.1.1.; The MathWorks, Inc.: Natick, MA, USA, 2010.
38. Maier, H.R.; Dandy, G.C. Neural networks for the prediction and forecasting of water resource variables: A review of modelling issues and applications. *Environ. Model. Softw.* **2000**, *15*, 101–124. [[CrossRef](#)]
39. Kaastra, I.; Boyd, M.S. Forecasting futures trading volume using neural networks. *J. Futures Mark.* **1995**, *15*, 953–970. [[CrossRef](#)]
40. Karunanithi, N.; Grenney, W.J.; Whitley, D.; Bovee, K. Neural networks for river flow prediction. *J. Comput. Civ. Eng.* **1994**, *8*, 201–220. [[CrossRef](#)]
41. Cigizoglu, H.K. Estimation, forecasting and extrapolation of river flows by artificial neural networks. *Hydrol. Sci. J.* **2003**, *48*, 349–361. [[CrossRef](#)]
42. Rezaeian-Zadeh, M.; Zand-Parsa, S.; Abghari, H.; Zolghadr, M.; Singh, V.P. Hourly air temperature driven using multi-layer perceptron and radial basis function networks in arid and semi-arid regions. *Theor. Appl. Climatol.* **2012**, *109*, 519–528. [[CrossRef](#)]
43. Hosseinzadeh Talae, P.; Tabari, H.; Sobhan Ardakani, S. Hydrological drought in the west of Iran and possible association with large-scale atmospheric circulation patterns. *Hydrol. Process.* **2014**, *28*, 764–773. [[CrossRef](#)]
44. Cheng, B.; Titterton, D.M. Neural networks: A review from a statistical perspective. *Stat. Sci.* **1994**, *9*, 2–54. [[CrossRef](#)]
45. Weigend, T. *Practical Neural Network Recipes in C++*; Academic Press: San Diego, CA, USA, 1993.
46. Weigend, A.S.; Rumelhart, D.E.; Huberman, B.A. Predicting the future: A connectionist approach. *Int. J. Neural Syst.* **1990**, *1*, 193–209. [[CrossRef](#)]
47. Amari, S.-I.; Murata, N.; Muller, K.-R.; Finke, M.; Yang, H.H. Asymptotic statistical theory of overtraining and cross-validation. *IEEE Trans. Neural Netw.* **1997**, *8*, 985–996. [[CrossRef](#)] [[PubMed](#)]
48. Sethi, R.R.; Kumar, A.; Sharma, S.P.; Verma, H.C. Prediction of water table depth in a hard rock basin by using artificial neural network. *Int. J. Water Resour. Environ. Eng.* **2010**, *2*, 95–102.
49. Adamowski, J.; Prasher, S. Comparison of machine learning methods for runoff forecasting in mountainous watersheds with limited data. *J. Water Land Dev.* **2012**, *17*, 89–97. [[CrossRef](#)]
50. Sharda, V.; Srivastava, P.; Ingram, K.; Chelliah, M.; Kalin, L. Quantification of El Niño Southern Oscillation (ENSO) impact on precipitation and stream flows for improved management of water resources in Alabama. *J. Soil Water Conserv.* **2012**, *67*, 158–172. [[CrossRef](#)]
51. Mo, K.C.; Schemm, J.E. Relationship between ENSO and drought over the Southeastern United States. *Geophys. Res. Lett.* **2008**, *35*, L15701. [[CrossRef](#)]
52. Lee, S.-K.; Mapes, B.E.; Wang, C.; Enfield, D.B.; Weaver, S.J. Springtime ENSO phase evolution and its relation to rainfall in the continental U.S. *Geophys. Res. Lett.* **2014**, *41*, 1673–1680. [[CrossRef](#)]
53. Mearns, L.O.; Giorgi, F.; Shields, C.; McDaniel, L. Climate scenarios for the southeastern US based on GCM and regional modeling simulations. *Clim. Chang.* **2003**, *60*, 7–36. [[CrossRef](#)]

54. Majidzadeh, H.; Wang, J.; Chow, A.T. Prescribed Fire Alters Dissolved Organic Matter and Disinfection By-Product Precursors in Forested Watersheds—Part I. A Controlled Laboratory Study. In *Recent Advances in Disinfection By-Products*; American Chemical Society: Washington, DC, USA, 2015; Chapter 15; pp. 271–292.
55. Todd, M.J.; Muneeppeerakul, R.; Miralles-Wilhelm, F.; Rinaldo, A.; Rodriguez-Iturbe, I. Possible climate change impacts on the hydrological and vegetative character of Everglades National Park, Florida. *Ecohydrology* **2012**, *5*, 326–336. [[CrossRef](#)]
56. Zhu, Q.; Peng, C.; Ciais, P.; Jiang, H.; Liu, J.; Bousquet, P.; Li, S.; Chang, J.; Fang, X.; Zhou, X.; et al. Interannual variation in methane emissions from tropical wetlands triggered by repeated El Niño Southern Oscillation. *Glob. Chang. Biol.* **2017**, *23*, 4706–4716. [[CrossRef](#)] [[PubMed](#)]
57. Erwin, K.L. Wetlands and global climate change: The role of wetland restoration in a changing world. *Wetlands Ecol. Manag.* **2009**, *17*, 71–84. [[CrossRef](#)]
58. Srivastava, N.; Hinton, G.; Krizhevsky, A.; Sutskever, I.; Salakhutdinov, R. Dropout: A simple way to prevent neural networks from overfitting. *J. Mach. Learn. Res.* **2014**, *15*, 1929–1958.



© 2018 by the authors. Licensee MDPI, Basel, Switzerland. This article is an open access article distributed under the terms and conditions of the Creative Commons Attribution (CC BY) license (<http://creativecommons.org/licenses/by/4.0/>).